Instability criteria and pattern formation in the complex Ginzburg-Landau equation with higher-order terms

Alidou Mohamadou,[1,2,3] Bebe Emilienne Ayissi,[1] and Timoléon Crépin Kofané[1,3]
[1]*Laboratory of Mechanic, Department of Physics, Faculty of Science, University of Yaoundé I, P.O. Box 812, Yaoundé, Cameroon*
[2]*Condensed Matter Laboratory, Department of Physics, Faculty of Science, University of Douala, P.O. Box 24157, Douala, Cameroon*
[3]*The Abdus Salam International Centre for Theoretical Physics, P.O. Box 586, Strada Costiera, 11, I-34014 Trieste, Italy*
(Received 16 March 2006; revised manuscript received 13 June 2006; published 5 October 2006)

We study the modulational instability and spatial pattern formation in extended media, taking the one-dimensional complex Ginzburg-Landau equation with higher-order terms as a perturbation of the nonlinear Schrödinger equation as a model. By stability analysis for the original partial differential equation, we derive its stability condition as well as the threshold for amplitude perturbations and we show how nonlinear higher-order terms qualitatively change the behavior of the system. The analytical results are found to be in agreement with numerical findings. Modulational instability mediates pattern formation through the lattice. The main feature of the traveling plane waves is its disintegration in pulse train during the propagation through the system.

DOI: 10.1103/PhysRevE.74.046604 PACS number(s): 05.45.Yv, 42.65.Tg, 89.75.Kd, 89.75.Fb

I. INTRODUCTION

For over 30 years now, it has been known that stable localized solutions can exist for certain nonlinear partial differential equations. The best-known example of such solutions is solitons, which are localized solutions that occur in purely dispersive systems such as the nonlinear Schrödinger (NLS) equation. The NLS equation is a universal model for nonlinear wave propagation that has been studied extensively in nonlinear optics. Of particular interest is the modulational instability (MI) and soliton propagation in nonlinear waveguides and optical fibers [1]. Recent investigations on the propagation of light pulses through optical fibers [1–3] and optical fiber laser [4,5] have aroused considerable interest in the study of the nonlinear effect described by the NLS and higher-order NLS equation [1,6,7] and higher-order complex Ginzburg-Landau equation [8–10]. The NLS equation with nonconservative terms added is usually called the complex Ginzburg-Landau (CGL) equation. During the past decade, the capacity of light wave systems was dramatically improved by the impressive developments in laser, amplifier, and fiber technologies as well as multiplexing techniques. The better understanding of the underlying physics will lead to the Tbyte/s operation regime in the next generation of ultrahigh-speed optical telecommunication systems [1,3]. High bit rates correspond to narrow pulse widths per channel. Thereby, new physical effects will become important in the system. When studying ultrashort pulses in optical fibers and optical fiber lasers, we realized that not only the value of the second-order dispersion is important, but also its slope (third-order dispersion), curvature (fourth-order dispersion), self-steepening, and self-frequency-shift arising from stimulated Raman scattering [1].

Dissipative systems are more complicated than Hamiltonian ones in the sense that, in addition to nonlinearity and dispersion, they include energy exchanged with an external source. The generic equation that describes dissipative systems above the point of bifurcation is the CGL equation and its different modifications [11–17]. A review of experiments described by the CGL equation is given in Refs. [16,17]. But the CGL equation with higher-order terms has been analyzed less extensively, except that Deissler and Brand [18] have studied numerically the effect of a nonlinear gradient term, and Thian *et al.* [19] have also investigated its exact analytical front solution. However, they are worth investigating further as mentioned by Saarloos and Hohenberg [20], since the more general model is useful for understanding various experimental phenomena. Another useful example, from the standpoint of possible applications, is the optical pulse transmission line. The propagation of picosecond optical pulses in optical fibers is approximately governed by the NLS equation. When frequency- and intensity-dependent gain and loss have to be taken into account for long-distance communication, the governing equation should be replaced by the cubic CGL equation [21]. When third-order dispersion is compensated, the equation to describe the propagation of ultrashort pulses will be reduced to the CGL equation with higher-order terms [19,20]. Stationary solutions to these equations can frequently be found by using both analytical and numerical methods. One of the fundamental problems left is to check these solutions against their stability, which is essential from a basic point of view as well as for potential applications. In particular, in nonlinear optics this question has attracted a considerable amount of interest during the past several years. Different kinds of instability may lead to such phenomena as phase turbulence, bistability, self-oscillation, and the formation of static or moving patterns. A prominent example is MI, which is the prerequisite for the formation of spatial or temporal patterns. In an optical fiber, MI of a continuous wave can be employed for the generation of pulse trains with high repetition rate [1,3]. Therefore, the aim of this paper is to study MI for plane waves moving across the system as well as the propagation of unstable patterns with high repetition rate. In Sec. II, we report the linear stability analysis of a plane-wave solution of the CGL equation with higher-order terms. The stability conditions as well as the threshold amplitude are presented. In the next section, the validity of analytical results is checked by numerical simulations. Section

IV is devoted to the study of different wave pattern formation that the nonlinear extended plane wave may display. We show how the presence of the higher-order term has profound consequences on the dynamics of the CGL equation. The last section concludes the paper.

II. THE MODEL AND LINEAR STABILITY ANALYSIS

In perturbative analysis of the microscopic equations for various systems, one encounters complex partial differential equations that go under the name of "amplitude equations." Considered in their own right as model dynamical systems, we will refer to them as Ginzburg-Landau models [22,23], a prototype of which is

$$\psi_t - (b_1 + ic_1)\nabla^2\psi + f_1(|\psi|^2)\psi, \tag{1}$$

where

$$f_l = f_{lr} + if_{li} \tag{2}$$

is an arbitrary complex function of its argument $|\psi|^2$, and b_1 and c_1 are real constants. In one dimension, we will also consider the generalized equation

$$\psi_t = (b_1 + ic_1)\psi_{xx} + f_1(|\psi|^2)\psi + \partial_x[f_2(|\psi|^2)\psi] + [\partial_x f_3(|\psi|^2)]\psi, \tag{3}$$

where f_2 and f_3 are complex functions. There are clearly many variants of the above equations, with anisotropic derivatives in higher dimensions, or with other fields coupled to ψ. The special case

$$f_1 = \varepsilon - (b_3 - ic_3)|\psi|^2 - (b_5 - ic_5)|\psi|^4, \tag{4}$$

with $\varepsilon = b_1 = b_3 = b_5 = c_5 = 0$, is the NLS equation

$$\partial_t\psi = ic_1\partial_x^2\psi + ic_3|\psi|^2\psi, \tag{5}$$

and the case $c_5 \neq 0$ we will call the quintic-cubic Schrödinger equation. In this case, Eq. (6) models transmission of optical pulses in a pumped dispersion-decreasing fiber or femtosecond light

$$\partial_t\psi = ic_1\partial_x^2\psi + ic_3|\psi|^2\psi + ic_5|\psi|^4\psi. \tag{6}$$

A model that has been studied in the plasma literature is the "derivative NLS" equation

$$b_1 = f_1 = f_3 = 0, \quad f_2(|\psi|^2) = s_0 + s_1|\psi|^2, \tag{7a}$$

$$\partial_t\psi = ic_1\partial_x^2\psi + \partial_x[(s_0 + s_1|\psi|^2)\psi]. \tag{7b}$$

One can also define a case called the "generalized derivative nonlinear Schrödinger" equation, obtained from Eq. (3) by assuming

$$b_1 = f_{1r} = f_{2i} = f_{3i} = 0, \tag{8}$$

namely

$$\partial_t\psi = ic_1\partial_x^2\psi + if_{1i}(|\psi|^2)\psi + \partial_x[f_{2r}(|\psi|^2)\psi] + \partial_x[f_{3r}(|\psi|^2)\psi]. \tag{9}$$

In this work, we deal with the generalized Ginzburg-Landau model considered in Refs. [16,18,20],

$$f_2 = (m_r + im_i)|\psi|^2, \tag{10a}$$

$$f_3 = (n_r + in_i)|\psi|^2, \tag{10b}$$

where b, c, m, and n are real constants. Then Eq. (3) becomes as follows:

$$\psi_t = \varepsilon\psi + (b_1 + ic_1)\psi_{xx} - (b_3 - ic_3)|\psi|^2\psi - (b_5 - ic_5)|\psi|^4\psi + (m_r - im_i)\partial_x(|\psi|^2\psi) + (n_r - in_i)\partial_x(|\psi|^2)\psi. \tag{11}$$

It is important to note the role of the Ginzburg-Landau equations as model equations. This equation is widespread in nonlinear physic due to its ubiquitous presence in natural phenomena. The CGL equation is also used as a test case for several techniques. Many properties of nonequilibrium systems are encountered in these equations, and indeed many hard problems, such as the existence and interaction of defects and coherent structures, or the appearance of chaos, may profitably be addressed in the simple framework provided by these equations. However, it is only as a perturbative expansion valid in a small region near threshold that they provide a qualitative description of real experimental systems, and results may be even qualitatively misleading if applied far from threshold.

If the last two terms on the right-hand side are neglected, Eq. (11) reduces to the quintic equation, whose dynamical behaviors have extensively been investigated (see, for example, Refs. [16,19,24,25]). Within the context of nonlinear optic, the discrete CGL (DCGL) equation arises in the description of semiconductor laser arrays [26,27], where the quintic term can account for the gain and nonlinear saturation of the lasing medium. The DCGL equation can also describe the dynamics of an open Bose-Einstein condensate. In this case, the lattice potential is created by the interference of two optical standing waves [28], and thus solitons of the DNLS equation are known to exist. The dissipation of the Bose-Einstein condensate naturally occurs in an open condensate, while gain can result from the interaction between the condensed and the uncondensed atoms [29,30]. As a physical system described by the quintic CGL equation, one may consider a soliton fiber with nonlinear polarization-dependent losses (which is equivalent to fast saturable absorption action [31–33]). In this case, the time-localized pulse is supported by the nonlinear gain and energy due to three effects: spectral filtering, linear losses, and the quintic stabilizing term. So a stable stationary soliton state may be formed as a result of the balance between nonlinear gain, spectral filtering, and the quintic stabilizing term. It is quite remarkable that, in the normal dispersion regime, the stable solutions of the cubic-quintic CGL equation exhibit an important qualitative agreement with the experimental observation of a nearly exponential growth of pulse energy with the absolute value of the average dispersion [34]. However, there are few corresponding studies in the presence of higher-order terms f_2 and f_3. Note that the model parameters are generally dependent on the selected physical systems. For propagation of nonlinear light pulses in optical systems, $\psi(x,t)$ is the complex envelope of the electric field, t is the normalized propagation distance, and x is the retarded time. The param-

eters $\varepsilon>0$ ($\varepsilon<0$) represent the linear gain (loss), c_1 is the group velocity dispersion, c_3 is the nonlinear Kerr effects, b_1 describes the effect of spectral limitation due to gain bandwidth-limited amplification and (or) spectral filtering [which are inversely proportional to gain and (or) spectral filtering bandwidth, respectively], b_3 accounts for the nonlinear gain [and (or) absorption] processes, b_5 and c_5 describe the saturable effects of the nonlinear gain [and (or) absorption] and nonlinear dispersion term, and n_r and n_i are the nonlinear gradient terms that result from the time-retarded induced Raman process. In fact, n_i is usually responsible for the self-frequency shift. Usually, m_i and n_r are neglected in optical transmission systems because they are much smaller than m_r and n_i.

As is well known, Eq. (11) may also be applied to describe stationary beam propagation in planar optical waveguides. In the latter case, the variable x stands for the transversal spatial coordinate. Equation (11) has an exact continuous-wave solution,

$$\psi(x,t)=\psi_0 e^{i\theta_0(x,t)},\quad \theta_0(x,t)=kx-\omega t, \tag{12}$$

in which the wave number k and the angular frequency ω of the carrier are constants satisfying

$$\omega=c_1k^2-(c_3+2m_r)|\psi_0|^2-c_5|\psi|^4, \tag{13a}$$

$$|\psi_0|^2=\frac{(2m_i-b_3)\pm\sqrt{(b_3-2m_i)^2-4b_5(b_1k^2-\varepsilon)}}{2b_5}. \tag{13b}$$

The nonlinear effects in the solution (12) deal with the fact that the amplitude $|\psi_0|^2$ is not arbitrary (as it is usually for the linear case) but is a specific function of the wave number [see relation (13b)] k, for positive values of the right-hand side of Eq. (13b) with the necessary condition $(b_3-2m_i)^2-4b_5(b_1k^2-\varepsilon)>0$.

To discuss the MI of the continuous solution (12) in the framework of the CGL equation in the presence of higher-order terms, we look for solutions of Eq. (11) in the form of small-amplitude excitations of the continuous-wave background,

$$\psi(x,t)=\psi_0[1+\phi(x,t)]\exp[i\theta_0(x,t)], \tag{14}$$

wherein $\phi(x,t)$ is a complex quantity. Assuming $\phi(x,t)\ll\psi_0$, we obtain the equation for the perturbation $\phi(x,t)$,

$$\phi_t=(b_1+ic_1)[\phi_{xx}+2ik\phi_x]-[(b_3-ic_3)-2(b_5-ic_5)|\psi_0|^2](\phi+\phi^*)|\psi_0|^2+(m_r+im_i)[3\phi_x+\phi_x^*+2ik(\phi+\phi^*)]|\psi_0|^2$$
$$+(n_r+in_i)(\phi_x+\phi_x^*)|\psi_0|^2, \tag{15}$$

where * denotes the complex conjugation. Solution of Eq. (15) can be found in the form

$$\phi(x,t)=\phi_1\exp[i(lx+\Omega t)]+\phi_2^*\exp[-i(lx+\Omega^* t)]. \tag{16}$$

In Eq. (16), ϕ_1 and ϕ_2 are complex constant amplitudes, and Ω and l represent the angular frequency and the wave number of the perturbation, respectively. The substitution of Eq. (16) into Eq. (15) leads to a linear homogeneous system for ϕ_1 and ϕ_2 defined by

$$(-i\Omega+a_{11})\phi_1+a_{12}\phi_2=0,$$

$$a_{21}\phi_1+(-i\Omega+a_{22})\phi_2=0, \tag{17}$$

in which

$$a_{11}=-(2kl+l^2)(b_1+ic_1)-[(b_3-ic_3)+2(b_5-ic_5)|\psi_0|^2]|\psi_0|^2+i[(3l+2k)(m_r+im_i)+l(n_r+in_i)|\psi_0|^2], \tag{18a}$$

$$a_{12}=-[(b_3-ic_3)+2(b_5-ic_5)|\psi_0|^2]|\psi_0|^2+i[(l+2k)(m_r+im_i)+l(n_r+in_i)|\psi_0|^2], \tag{18b}$$

$$a_{21}=-[(b_3+ic_3)+2(b_5+ic_5)|\psi_0|^2]|\psi_0|^2-i[(-l+2k)(m_r-im_i)-l(n_r-in_i)|\psi_0|^2], \tag{18c}$$

$$a_{22}=(2kl-l^2)(b_1-ic_1)-[(b_3+ic_3)+2(b_5+ic_5)|\psi_0|^2]|\psi_0|^2-i[(2k-3l)(m_r-im_i)-l(n_r-in_i)|\psi_0|^2]. \tag{18d}$$

The condition for the existence of nontrivial solutions of system (17) gives rise to a second-order equation for the frequency Ω that represents the dispersion law for the perturbation,

$$\Omega^2+\alpha\Omega+\beta=0, \tag{19}$$

where

$$\alpha=i(a_{11}+a_{22})\ \text{and}\ \beta=a_{12}a_{21}-a_{11}a_{22}. \tag{20}$$

The expression of the discriminant (delta) of Eq. (19) is

$$\Delta = A + iB \tag{21}$$

with

$$A = [2c_1kl - (n_r + 3m_r)l|\psi_0|]^2 - [l^2b_1 + (b_3 + 2km_i + 2b_5|\psi_0|^2)|\psi_0|^2]^2 - (b_1^2 + c_1^2)[(2kl)^2 - l^4] + 8l^2(m_r^2 + m_i^2)|\psi_0|^4 + 2l^2(b_3b_1 - c_3c_1)|\psi_0|^2 + 4l^2(b_1b_5 - c_1c_5)|\psi_0|^2 + 4kl^2(n_rc_1 - n_ib_1)|\psi_0|^2 - 8kl^2(m_rc_1 - m_ib_1)|\psi_0|^2 - 4l^2(m_in_i + m_rn_r)|\psi_0|^4, \tag{22}$$

$$B = -2[2c_1kl - (n_r + 3m_r)l|\psi_0|^2][l^2b_1 + b_3 + 2km_i + 2b_5|\psi_0|^2]|\psi_0|^2 + 4kl[(b_3c_1 + c_3b_1) + 2(b_5c_1 + c_5b_1)|\psi_0|^2]|\psi_0|^2 + 2l(4k^2 - 3l^2)(m_rb_1 + m_ic_1)|\psi_0|^2 - 2l^3(n_rb_5 + n_ic_1)|\psi_0|^2 - 4l(m_rb_3 - m_ic_3)|\psi_0|^4 - 8l(m_rb_5 - m_ic_5)|\psi_0|^6 + 4l(n_rb_5 - n_ic_5)|\psi_0|^6. \tag{23}$$

The solutions of Eq. (19) are given by the following complex quantities:

$$\Omega_1 = \gamma + i\eta + (A + iB)^{1/2}, \tag{24a}$$

$$\Omega_1 = \gamma + i\eta - (A + iB)^{1/2}, \tag{24b}$$

where

$$\gamma = 2c_1kl - (n_r + 3m_r)l|\psi_0|^2,$$

$$\eta = -[l^2b_1 + (b_3 + 2km_i + 2b_5|\psi_0|^2)|\psi_0|^2]. \tag{25}$$

To continue, we shall distinguish two cases each related to the sign of B. So, when $B<0$, the roots of Δ (i.e., h_1 and h_2) help to put the frequencies Ω_1 and Ω_2 in the explicit form

$$\Omega_1 = \gamma + i\eta + h_1 - ih_2 = (\gamma + h_1) + i(\eta - h_2), \tag{26a}$$

$$\Omega_2 = \gamma + i\eta - h_1 - ih_2 = (\gamma - h_1) + i(\eta + h_2), \tag{26b}$$

in which

$$h_1 = \sqrt{\frac{1}{2}(A + \sqrt{A^2 + B^2})} \quad \text{and} \quad h_2 = \sqrt{\frac{1}{2}(-A + \sqrt{A^2 + B^2})}. \tag{27}$$

In the case $B>0$, the solutions of Eq. (19) are now defined by the following expressions:

$$\Omega_1' = \gamma + i\eta - h_1 - ih_2 = (\gamma - h_1) + i(\eta - h_2), \tag{28a}$$

$$\Omega_2' = \gamma + i\eta + h_1 + ih_2 = (\gamma + h_1) + i(\eta + h_2), \tag{28b}$$

and lead to solutions that have the same asymptotic behavior as those derived from relations (26a) and (26b). Due to the fact that Ω_1 and Ω_2 are complex quantities, it is not easy to give their sign. But their imaginary parts contribute to increase the effects of perturbation in the system. Substitution of Eq. (26a) into Eq. (16) enables us to understand the behavior of $\psi(x,t)$. Because h_2 is positive, $\eta - h_2 < \eta + h_2$ always holds and then this behavior is a function of the sign of $\eta - h_2$, which represents the imaginary part of Ω_1. Indeed, we have

$$\phi_1 e^{i\Omega t} = \phi_1 e^{i\Omega_1 t} = \phi_1 e^{i(\gamma + h_1)t} x e^{-(\eta - h_2)t} = \phi_1 e^{i(\gamma + h_1)t} x e^{(h_2 - \eta)t}. \tag{29}$$

Hence, it becomes clear that the asymptotic behavior of Eq. (16) depends on the sign of the constant $\eta - h_2$. If $\eta<0$, then $h_2 - \eta$ is always greater than zero and Eq. (16) increases exponentially when t tends to infinity. The system remains unstable under the modulation. But, if $\eta>0$, the behavior of Eq. (16) will depend on the sign of the quantity $h_2 - \eta$. Two situations appear and are discussed below.

(i) When $h_2 - \eta > 0$, i.e., $\eta - h_2 < 0$, i.e., $\mathrm{Im}(\Omega_1) < 0$. (30)

The solution (16) diverges without limit as t increases and the system is said to be modulationally unstable. Therefore, the difference $\eta - h_2$ can be written as

$$\eta - h_2 = \eta - \left(\frac{1}{2}\{-[2c_1kl - (n_r + 3m_r)l|\psi_0|^2]^2 - (b_1^2 + c_1^2)l^4 - 8l^2(m_r^2 + m_i^2)|\psi_0|^4 - 2l^2(b_3b_1 - c_3c_1)|\psi_0|^2 - 4l^2(b_1b_5 - c_5c_1)|\psi_0|^4 + 4kl^2(n_rc_1 - n_ib_1)|\psi_0|^2 + 8kl^2(m_rc_1 - m_ib_1)|\psi_0|^2 + 4l^2(m_in_i + m_rn_r)|\psi_0|^4 + h_0\}\right)^{1/2} \tag{31}$$

with

$$h_0 = [l^2 b_1 + (b_3 + 2km_i + 2b_5|\psi_0|^2)|\psi_0|^2]^2 + (b_1^2 + c_1^2)(2kl)^2 + (A^2 + B^2)^{1/2}. \tag{32}$$

We should stress that the quantity h_0 is a positive constant. Hence, we have

$$\eta - h_2 \leq \eta - \left(\frac{1}{2}\{-[2c_1kl - (n_r + 3m_r)l|\psi_0|^2]^2 - (b_1^2 + c_1^2)l^4 - 8l^2(m_r^2 + m_i^2)|\psi_0|^4 - 2l^2(b_3b_1 - c_3c_1)|\psi_0|^2 - 4l^2(b_1b_5 - c_5c_1)|\psi_0|^4 + 4kl^2(n_rc_1 - n_ib_1)|\psi_0|^2 + 8kl^2(m_rc_1 - m_ib_1)|\psi_0|^2 + 4l^2(m_in_i + m_rn_r)|\psi_0|^4\}\right)^{1/2}. \tag{33}$$

We can note that the inequality $\mathrm{Im}(\Omega_1) < 0$ is satisfied as soon as we have

$$\eta - \left\{\frac{1}{2}[-2l^2(b_3b_1 - c_3c_1)|\psi_0|^2 - 4l^2(b_1b_5 - c_5c_1)|\psi_0|^4 + 4kl^2(n_rc_1 - n_ib_1)|\psi_0|^2 + 8kl^2(m_rc_1 - m_ib_1)|\psi_0|^2 + 4l^2(m_in_i + m_rn_r)|\psi_0|^4 + h_3]\right\}^{1/2} < 0, \tag{34}$$

with

$$h_3 = -[2c_1kl - (n_r + 3m_r)l|\psi_0|^2]^2 - 8l^2(m_r^2 + m_i^2)|\psi_0|^4 - (b_1^2 + c_1^2)l^4. \tag{35}$$

Since η is a positive quantity, arrangements of Eq. (34) yield

$$(b_3b_1 - c_3c_1) - r < -\left(\frac{2\eta^2 - h_3}{2l^2|\psi_0|^2}\right) < 0 \tag{36}$$

and necessarily

$$(b_3b_1 - c_3c_1) + [2(b_1b_5 - c_5c_1)|\psi_0|^2] - r < 0, \tag{37}$$

in which the quantity r is given by

$$r = 2k(n_rc_1 - n_ib_1) + 4k(m_rc_1 - m_ib_1) + 2(m_in_i + m_rn_r)|\psi_0|^2. \tag{38}$$

Equation (37) represents the MI criterion for Stokes waves in physical systems described by the CGL equation with higher-order terms. Moreover, the relation (37) is the well-known Lange and Newell criterion [35,36]. From Eq. (38), we remark that the corrective term r depends on the characteristic parameters of the carrier wave $(k, |\psi_0|^2)$. Dealing with the work of Lange and Newell [35] for $r=0$, it should be remembered that harmonic waves are subcritical for $c_1c_5 - b_1b_5 > 0$ and are supercritical for $c_1c_5 - b_1b_5 < 0$.

Now, we deduce from Eq. (38) that if $r > 0$, then all supercritical waves are unstable under the modulation and subcritical waves with $r > c_1c_5 - b_1b_5 > 0$ are also unstable. Figure 1(a) plots regions of instability in the (m_r, n_r) plane. Black areas represent the place where the system develops an instability. The criterion (37) depends on the amplitude $|\psi_0|^2$. This fact allows us to determine the threshold amplitude of an unstable monochromatic wave for a given wave number, viz.,

$$|\psi_0|^2 > |\psi_{0,\mathrm{cr}}|^2 = \frac{(b_1b_3 - c_1c_3) + 2k(n_rc_1 - n_ib_1) - 4k(m_rc_1 - m_ib_1)}{2[(c_1c_5 - b_1b_5) + (m_in_i + m_rn_r)]}. \tag{39}$$

From Eq. (39), we see that a plane wave will be unstable to any modulation provided that the initial amplitude $|\psi_0|^2$ exceeds the threshold $|\psi_{0,c}|^2$ defined by Eq. (39). The corresponding threshold amplitude $|\psi_{0,c}|^2$ is depicted in Fig. 1(b) as a function of higher-order terms m_r and n_r.

(ii) On the other hand, previous calculations are exploited to establish from the condition $\eta - h_2 > 0$ [i.e., $\mathrm{Im}(\Omega_1) > 0$] that

$$(b_3b_1 - c_3c_1) + [2(b_1b_5 - c_5c_1)|\psi_0|^2] - r > 0, \tag{40}$$

This means that Stokes waves that satisfy the condition (40) are stable under modulation. We deduce from Eq. (40) that if $r < 0$, all subcritical waves are stable and supercritical waves with $r < c_1c_5 - b_1b_5 < 0$ are also stable under the modulation.

For the sake of comparison, the MI criterion (37) established in this work is quite similar to that obtained by Descalzi *et al.* [37] during their study of thermodynamic potentials for nonequilibrium systems. Furthermore, result (38) is interesting because the present approach to its investigation is very different from the method based on the Lyapunov functional developed by Descalzi *et al.* [37] and also from the method of cumulative momentum used by Lange and Newell [35].

III. NUMERICAL SIMULATIONS AND INFLUENCE OF HIGHER-ORDER TERMS

Linear stability analysis can only determine the onset of instability and predict qualitatively how the amplitude of the modulation wave with any perturbation wave numbers grows at the initial stage of instability. Moreover, linear approximation around carrier waves must fail for long time scales when the exponentially growing amplitude of unstable modulation wave is no longer small in comparison with that of the carrier wave. In order to check the validity of our analytical approach and to determine the evolution of the system beyond the instability point, we have performed numerical simulations of the CGL equation with higher-order terms. The fourth-order Runge-Kutta scheme is used to integrate Eq. (11). Most of the simulations are performed with a sys-

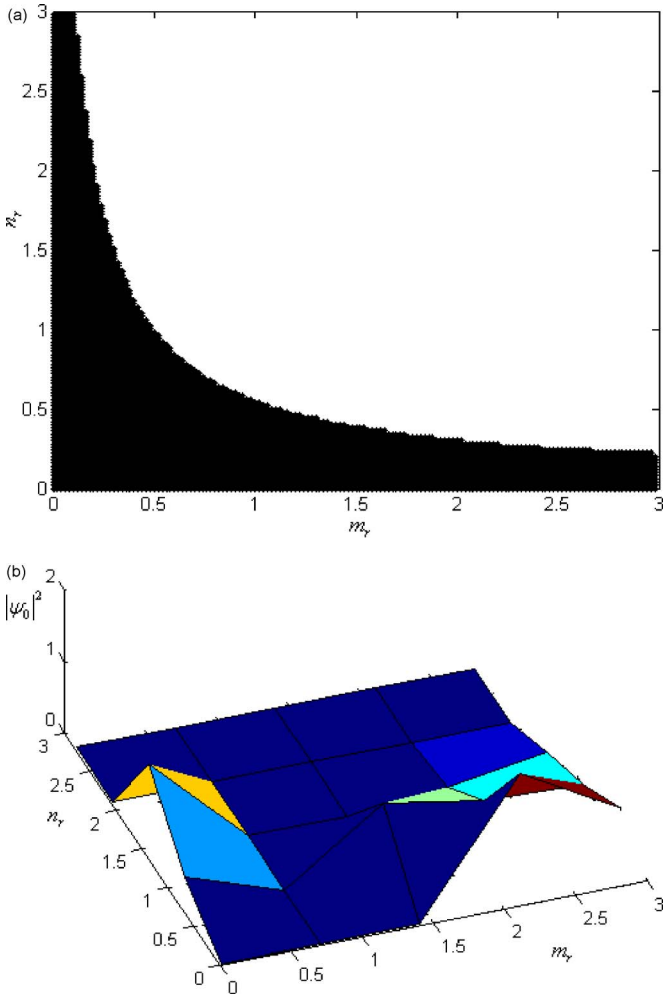

FIG. 1. (Color online) (a) Region of modulational instability in the (m_r,n_r) plane. The black areas are unstable. $c_1=0.1$, $b_1=0.5$, $c_3=0.2$, $b_3=0.9$, $c_5=1.0$, $b_5=0.7$, $m_i=-0.02$, $n_i=0.01$, and $\varepsilon=1.0$. (b) Threshold amplitude $c_1=2.5$, $b_1=0.125$, $c_3=0.2$, $b_3=0.09$, $c_5=0.75$, $b_5=0.07$, $m_i=1.02$, $n_i=0.025$, and $\varepsilon=1.0$.

tem involving N sites with $N=256$ with periodic boundary conditions. The accuracy of numerical experiments is examined by testing different time and space steps. Typically, the mesh sizes are chosen equal to $\Delta t=0.055$ and $\Delta x=0.5$. The wave numbers k and l have the form $k=2\pi p/N$ and $l=2\pi P/N$, where p and P are integers lower than $N/2$.

The initial conditions, which are typically at time $t=0$, are obtained by using a complex wave function that can be written as

$$\psi(t,x)=\psi^{\mathrm{Re}}(t,x)+i\psi^{\mathrm{Im}}(t,x). \tag{41}$$

Here, the upper indexes Re and Im stand for the real and imaginary part, respectively. We start from a solution of Eq. (11) as a plane wave of wave number k, with an amplitude that is perturbed by a modulation plane wave with wave number l since we are interested in MI. Thus initially, in our numerical simulation, the real and the imaginary parts of the wave function of the plane wave are coherently modulated in the form

$$\psi^{\mathrm{Re}}(0,x)=[\psi_0+\eta\cos(lx)]\cos(kx), \tag{42a}$$

$$\psi^{\mathrm{Im}}(0,x)=[\psi_0+\eta\cos(lx)]\sin(kx). \tag{42b}$$

This initial condition is therefore a modulated plane wave with amplitude ψ_0, which is derived from the preceding section [Eq. (13b)] and the modulation amplitude $\eta\ll\psi_0$. So, using the initial condition given in Eq. (42) has revealed that in this simple coherent modulation form of the amplitude, this initial condition allows us to study the response of the system separately for each modulation wave number.

As it is usually performed in a discrete lattice, we will study here the behavior of the system with the help of the spatial Fourier transform of $\psi(t,x)$,

$$m(p,t)=\int_{x=0}^{L}\psi(t,x)e^{i(2\pi xp/L)}. \tag{43}$$

In nonlinear physical systems, nonlinearity can create additional modulations. Indeed, an initial linear wave $\psi(0,x)=A\cos(kx)$ chosen as an initial condition will immediately create from the cubic nonlinearity a nonlinear component $\cos^3(kx)$. As

$$\psi(0,x)=A\cos(kx)+d\cos^3(kx)=\left[A+\frac{d}{2}[1+\cos(2kx)]\right]\cos(kx). \tag{44}$$

A modulation with a wave number $l=2k$ is immediately generated and should be taken into account to predict the stability. These modulations were forgotten in the analytical study of MI. Modulations that are generated by nonlinearity have very small amplitudes and we can forget them when the system is stable [38]. Of course when the system is in the unstable regime, we must take them into account because they will grow and finally play a crucial role. In order to study the impact of higher-order terms, we will present the growth rate of each individual Fourier component obtained by the least-square fitting of $|m(p,t)|^2$ over the first few periods during which the time is expected to grow at the rate of $h_2-\eta$.

Figure 2 shows the time evolution of the carrier wave with wave number $k=\pi/16$ modulated by small-amplitude waves with wave numbers $l=\pm\pi/4$. Figures 2(a) and 2(b) correspond to the particular case in which the higher-order terms are omitted: $m_r=m_i=n_r=n_i=0$. Here, Eq. (11) becomes the cubic-quintic Ginzburg-Landau equation [16,25,28]. The physical parameters are $c_1=-3.0$, $b_1=1.0$, $c_3=0.275$, $b_3=0.77$, $c_5=2.05$, $b_5=0.75$, and $\varepsilon=1.5$ in Fig. 2(a), while in Fig. 2(b) they are equal to $c_1=-3.0$, $b_1=1.0$, $c_3=0.275$, $b_3=0.77$, $c_5=0.75$, $b_5=0.1$, and $\varepsilon=1.5$. According to the instability criterion (37), the system is predicted to be unstable for these parameters. This is effectively verified numerically in the log-linear plot of Figs. 2(a) and 2(b), in which the modulation $3k$, which is not taken into account in the initial conditions, displays an exponential decrease at the beginning. The magnitude of component $3k$ is the highest one at the beginning. One can see that the $k-1$ component, which was neglected in the linear stability analysis, evolves with the same amplitude as the one of the carrier wave k. We also observe that, around units of time in Fig. 2(a) and 50 units of

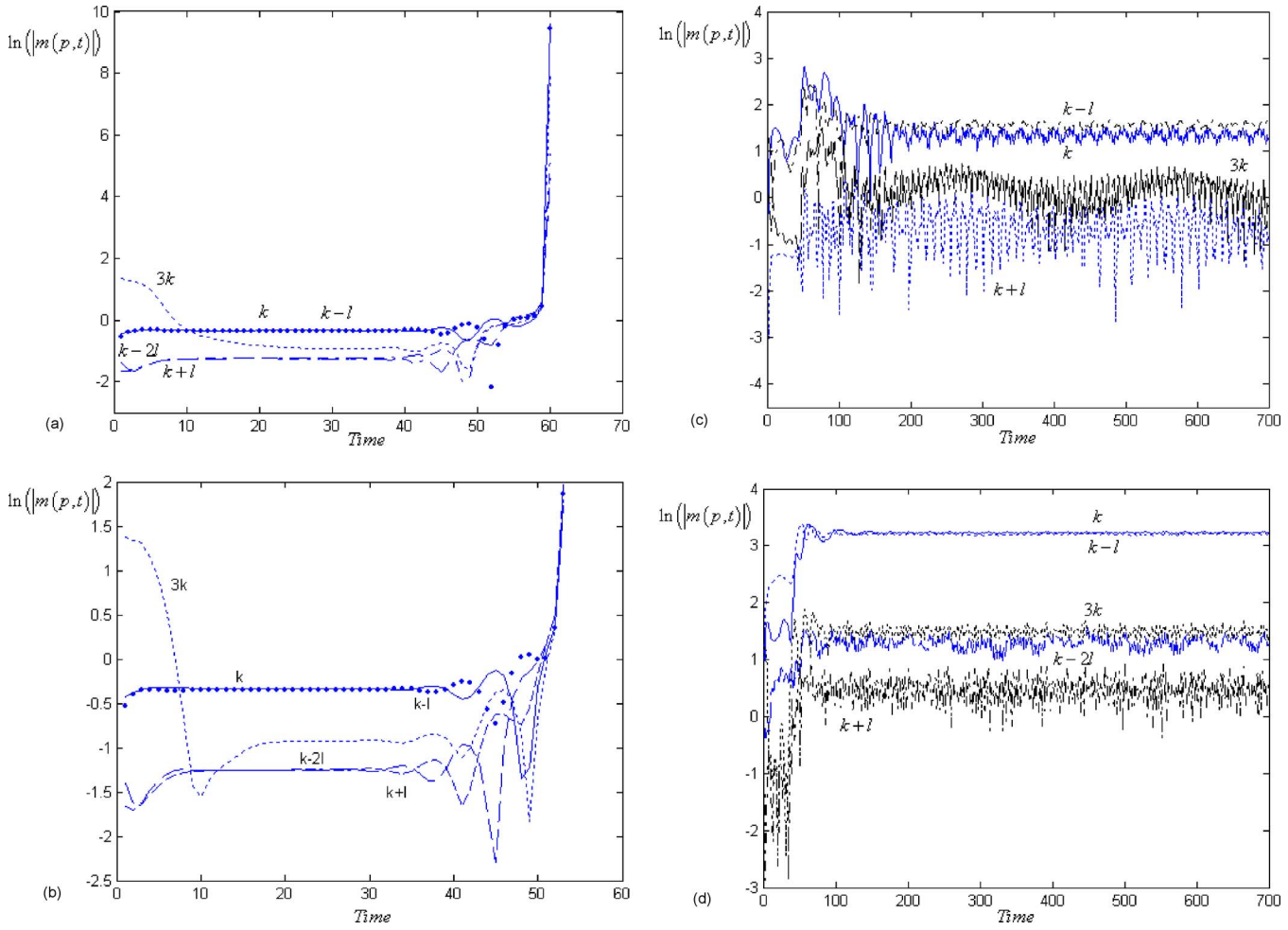

FIG. 2. (Color online) Time evolution of the amplitude of the Fourier transform for different parameters. (a) Time evolution of the amplitude in the absence of higher-order terms for the parameters: $c_1=-3.0$, $b_1=1.0$, $c_3=0.275$, $b_3=0.77$, $c_5=2.05$, $b_5=0.1$, and $\varepsilon=1.5$ for the wave number $k=\pi/16$ modulated at wave number $l=\pi/4$. (b) Time evolution of the amplitude in the absence of higher-order terms for the parameters $c_1=-3.0$, $b_1=1.0$, $c_3=0.275$, $b_3=0.77$, $c_5=0.75$, $b_5=0.1$, and $\varepsilon=1.5$ for the wave number $k=\pi/16$ modulated at wave number $l=\pi/4$. (c) Time evolution of the amplitude in the presence of higher-order terms. Same parameters as in (a) but with $m_r=0.01$, $m_i=0.01$, $n_r=0.05$, and $n_i=0.03$. (d) Time evolution of the amplitude in the presence of higher-order terms. Same parameters as in (b) but with $m_r=0.01$, $m_i=0.01$, $n_r=0.05$, and $n_i=0.025$.

time in Fig. 2(b), all the different modes and combination modes suddenly display a large increasing behavior of their amplitudes. At this stage, a buildup of the combination modes is obtained and the system becomes chaotic. This behavior is justified by the fact that, although the linear stability analysis neglects additional combination mode waves generated through wave-mixing processes, these, albeit small at the initial stage, can become significant and drive the system into a chaotic regime when the time increases if the wave numbers fall in an unstable domain.

Now, we take into consideration higher-order terms in the simulations. Figures 2(c) and 2(d) present the prolonged simulation of Figs. 2(a) and 2(b), respectively. At first glance, one can see that the higher-order terms have canceled the exponential growth of the amplitude obtained in Figs. 2(a) and 2(b). Stability can be achieved if one adds higher-order terms in the system. As the system is supposed to be unstable, we see that the magnitude of the combination mode $(k-l)$ can become the highest one [Fig. 2(c)] or reach the magnitude of the carrier wave [Fig. 2(d)]. We also see in Fig. 2(c) that the magnitude of the wave oscillates. While the magnitude of the k and $k-1$ components oscillates with an ultrashort wavelength, one of the $3k$ and $k+1$ components oscillates with a short wavelength. The reason is that the initial condition (42) does not take into account the correction on the phase [38,39].

IV. PATTERN FORMATION OF THE MODEL UNDER STUDY

Localized wave packets in linear media have a natural tendency to change their shape and broaden as they propagate, since the modes they are composed of propagate at different phase velocities. In nonlinear media, this broadening can be counteracted, resulting in a pulse/beam that does not change its shape during propagation: a soliton [40]. The notion of a soliton belongs to the most popular concepts in physics. Solitons are formed because of the existence of non-

linear interaction in the system, which cancels the dispersion and hence allows for the propagation of shape-preserving objects. In the case of dilute atomic quantum gases, the nonlinearity is determined by the effective interaction between atoms that can be both repulsive and attractive, while in optics, solitons can be understood as a balance between diffraction (in the spatial domain) or dispersion (in the time domain) and nonlinear self-focusing. Solitary solutions (solitons) are an important class of solution of nonlinear equations. There is an important difference between soliton solutions of Hamiltonian systems and autosoliton solutions in nonconservative systems [41]. In Hamiltonian systems, soliton solutions appear as a result of a balance between nonlinearity and dispersion, and these solutions usually comprise a one-parameter family. The generation of autosolitons is possible when two conditions—the equilibrium between nonlinearity and dispersion and the equilibrium between dissipation and amplification—are met. The solution satisfying these requirements simultaneously exists for fixed parameters defined by parameters of the equation. For envelope waves, autosolitons are described by the complex Ginzburg-Landau equation, which in some limit can be transformed to the nonlinear Schrödinger equation with complex perturbation. Closely related to the interplays between nonlinearity and dispersion is the process of MI. It is a symmetry-breaking instability so that a small perturbation on top of a constant amplitude background experiences exponential growth, and this leads to wave breakup in either space or time. These disintegrations have an envelope function with shape familiar to the theory of a solitonlike object. While MI is a crucial issue for soliton instability [1], it is also considered as a precursor to solitons formation because it typically occurs in the same parameter region as that where solitons are observed [1].

In this section, we examine for a variety of equation parameters the nature of different wave pattern formation that may be raised up by a MI process in the CGL equation with higher-order terms. Recently, a first example of MI mediated pattern formation in an anharmonic lattice was reported by Burlakov [42]. The reason for the pattern stability is shown to be closely related to interference of modulation instabilities of constituent spatial modes. We then continue by using the definition of a wave number given above (i.e., $k=2\pi p/N$ and $l=2\pi P/N$) for the carrier wave and the modulation wave. The system is now made up of 700 sites and we use the initial condition given by Eq. (42). Now, we look at the feature of our initial modulated wave through the system. As a first example, let us consider the parameters $c_1=1.0$, $b_1=-3.0$, $c_3=0.275$, $b_3=0.77$, $c_5=0.10$, $b_5=1.05$, $n_r=0.5$, $\varepsilon=1.5$, $m_r=m_i=n_i=0$, $k=4\pi/175$, and a long-wavelength modulation $l=4\pi/35$. According to the modulational instability criterion (37), the system is expected to develop an instability for these parameters. We observe in Fig. 3(a) that the amplitude of the wave displayed by wave motion is modulated in terms of a train of small-amplitude short waves. The wavelength of the train is not uniform along the chain. At the beginning of the system, the train has an ultrashort wavelength that increases at the middle and then decreases at the end. If we take into account the higher-order terms that were equal to zero ($m_r=0.01$, $m_i=0.01$, and $n_i=0.03$), the dynamics of the system changes, as we can see in Fig. 3(b). The number of trains increases in the system. Each element of the train has the shape of a soliton object. A soliton forms when the localized wave packet induces a potential (via the nonlinearity) and "captures" itself in it, thus becoming a bound state in its own induced potential. In the spatial domain of optics, a spatial soliton forms when a very narrow optical beam induces (through self-focusing) a waveguide structure and guides itself in its own induced waveguide. The relation between MI and solitons is best manifested in the fact that the filaments (or pulse trains) that emerge from the MI process are actually trains of almost ideal solitons. Therefore, MI can be considered to be a precursor to solitons formation. Now, from the parameters of Fig. 3(a) we increase the value of the saturable effects of nonlinear gain (b_5), which is now equal to 2.05. The wavelength of the pulse train increases while its amplitude de-

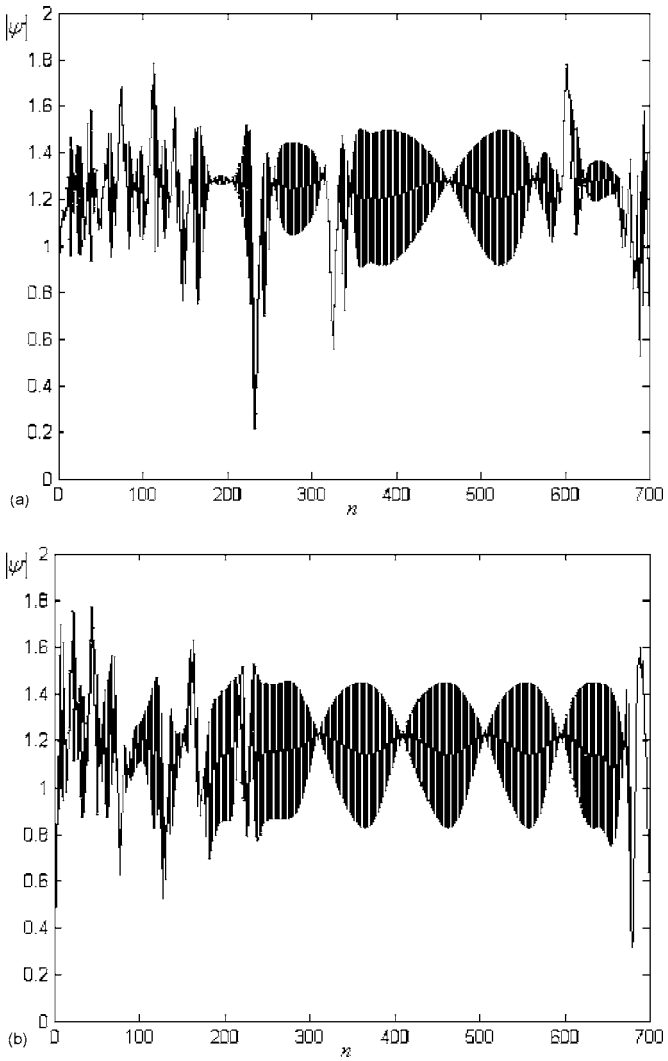

FIG. 3. MI leads to solitonlike object. (a) Disintegration of waves in filament which have the shape of a soliton for the parameters $c_1=1.0$, $b_1=-3.0$, $c_3=0.275$, $b_3=0.77$, $c_5=0.10$, $b_5=1.05$, $\varepsilon=1.5$, and $n_r=0.5$ for the wave number $k=\pi/32$ and $l=4\pi/35$. (b) Effect of higher-order terms on the propagation of pulse train: $m_r=0.01$, $m_i=0.01$, and $n_i=0.03$.

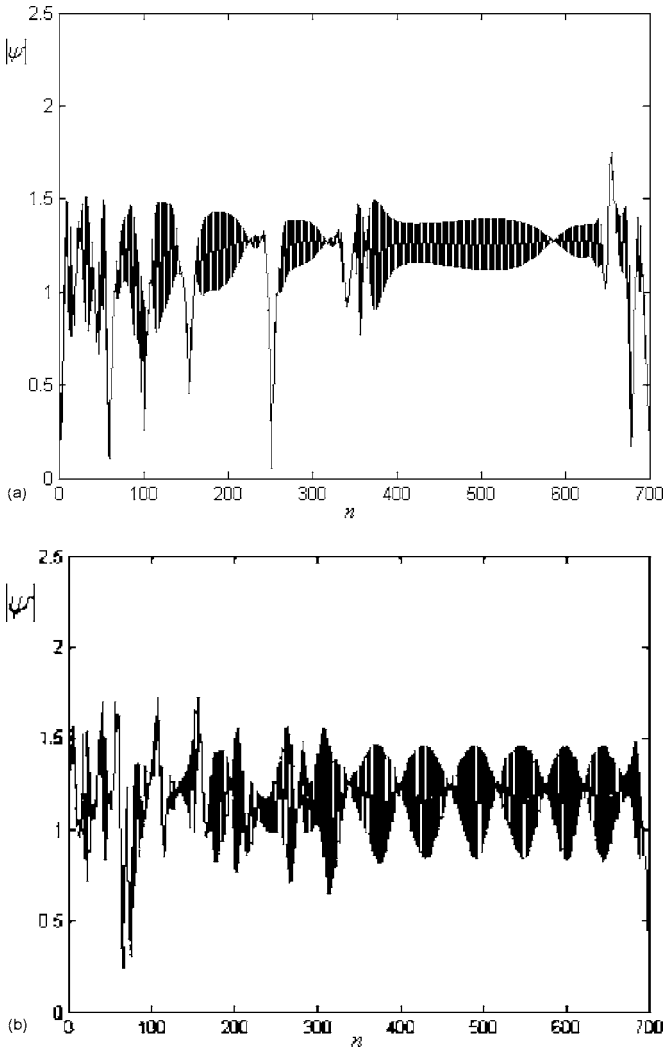

FIG. 4. Dependence of wave train on the saturable effects of nonlinear gain term b_5. (a) Propagation of wave packets, same parameters as in Fig. 3(a) but for $b_5=2.05$. (b) Propagation of wave packets, same parameters as in Fig. 3(b) but for $b_5=2.05$, $n_i=0.025$.

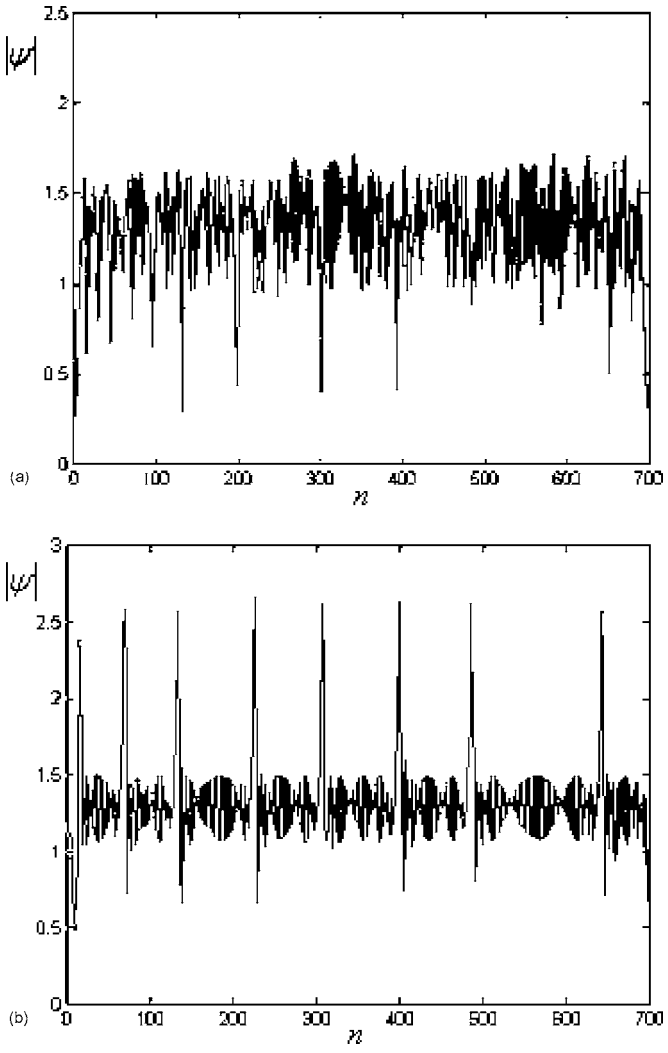

FIG. 5. Wave train. (a) Chaotic pulse train for the parameters $c_1=1.0$, $b_1=-3.0$, $c_3=0.275$, $b_3=0.77$, $c_5=0.25$, $b_1=0.75$, $\varepsilon=1.5$, $m_r=0.5$, and $m_i=n_r=n_i=0$ for the wave numbers $k=4\pi/175$ and $l=4\pi/35$. (b) Stabilization of pulse train by higher-order terms: $m_i=0.01$, $n_r=0.5$, and $n_i=0.025$.

creases, as one can see in Fig. 4(a). When the other higher-terms are present in the system, we obtain a chaotic pulse train at the beginning, and thereafter the pulse train becomes uniform. The number of pulse trains has increased here [Fig. 4(b)] and each of them has the shape of a soliton object with a short wavelength. As a last example, let us consider $c_1=1.0$, $b_1=-3.0$, $c_3=0.275$, $b_3=0.77$, $c_5=0.25$, $b_5=0.75$, $\varepsilon=1.5$, $m_r=0.5$, $m_i=n_r=n_i=0$, $k=4\pi/175$, and a long-wavelength modulation $l=4\pi/35$. The MI criterion (37) is also fulfilled for these sets of parameters. The wave pattern displayed by Fig. 5(a) is that of a chaotic pulse train. The wave moves with an ultrashort wavelength while the amplitude of the train fluctuates randomly. If we consider the higher-order terms, we see that the pulse train becomes uniform [Fig. 5(b)]. As in the previous section, we can see that the higher-order terms have stabilized the dynamic of the system.

V. CONCLUSION

We have revisited the MI and propagation of unstable pattern within the framework of the complex Ginzburg-Landau equation with higher-order terms. Based on this equation and exploiting the Stokes wave analysis, the well known Lange and Newell criterion for stability (instability) has been performed. We have obtained that the criterion depends on the sign of the quantity $\{(b_3b_1-c_3c_1)+[2(b_1b_5-c_5c_1)|\psi_0|^2]-r\}$ in which r represents the corrective term. The analytical results are compared to numerical simulations and good agreement is obtained. Since the long-time evolutions of nonlinear waves are analytically untractable, numerical simulations are employed. It reveals that combination waves generated via wave-mixing processes can have significant effects on the dynamic of the system. Higher-order terms have been used to stabilize the system. MI mediated

pattern formation in nonconservative terms has been described. One of the main effects of MI is the disintegration of waves into a pulse train, which has the shape of solitonlike objects. These pulse trains have been obtained in the present study. It would be interesting to check the predictions experimentally. Candidates include binary fluid convection, electroconvection in nematic liquid crystals, and high-capacity optical communications.

[1] G. P. Agrawal, *Nonlinear Fiber Optics* (Academic Press, San Diego, 2001).

[2] N. N. Akhmediev and A. Ankiewicz, *Solitons: Nonlinear Pulses and Beams* (Chapman and Hall, London, 1997).

[3] A. Hasegawa and Y. Kodama, *Soltons in Optical Communications* (Oxford University Press, Oxford, 1995).

[4] C. J. Chen, P. K. A. Wai, and C. R. Menyuk, Opt. Lett. **19**, 198 (1994); **20**, 350 (1995).

[5] J. M. Soto-Crespo and L. Pesquera, Phys. Rev. E **56**, 7288 (1997).

[6] Li Zhonghao, Li Lu, T. Huiping, and Z. Guosheng, Phys. Rev. Lett. **84**, 4096 (2000).

[7] T. Jinping *et al.*, Phys. Scr. **67**, 325 (2003).

[8] J. M. Soto-Crespo, N. N. Akhmediev, and V. V. Afanasjev, Opt. Commun. **118**, 587 (1995).

[9] Y. S. Kivshard and B. A. Malomed, Rev. Mod. Phys. **61**, 763 (1989).

[10] T. Huiping *et al.*, Appl. Phys. B **78**, 199 (2004).

[11] L. C. Crasovan, B. A. Malomed, D. Mihalahe, D. Mazilu, and F. Lederer, Phys. Rev. E **62**, 1322 (2000).

[12] P. Kolodner, Phys. Rev. A **44**, 6448 (1991).

[13] P. A. Belanger, L. Gagnon, and C. Paré, Opt. Lett. **14**, 943 (1989).

[14] Y. Kuramoto, *Chemical Oscillations, Waves and Turbulence* (Springer-Verlag, Berlin, 1984).

[15] C. Normand and Y. Pomeau, Rev. Mod. Phys. **49**, 581 (1993).

[16] M. C. Cross and P. C. Hohenberg, Rev. Mod. Phys. **65**, 851 (1993).

[17] I. S. Aranson and L. Kramer, Rev. Mod. Phys. **74**, 99 (2002).

[18] R. J. Deissler and H. R. Brand, Phys. Rev. Lett. **81**, 3856 (1998).

[19] H. Tian, Z. Li, J. Tian, and G. Zhou, Phys. Rev. E **66**, 066204 (2002).

[20] W. van Saarloos and P. C. Hohenberg, Physica D **56**, 303 (1992); W. van Saarloos, Phys. Rev. A **37**, 211 (1988); **39**, 6367 (1989).

[21] J. J. Hegseth, C. D. Andereck, F. Hayot, and Y. Pomeau, Phys. Rev. Lett. **62**, 257 (1989).

[22] V. L. Ginzburg and L. D. Landau, Zh. Eksp. Teor. Fiz. **20**, 1064 (1950).

[23] K. Stewartson and J. T. Stuart, J. Fluid Mech. **48**, 529 (1971).

[24] A. J. Kenfack and T. C. Kofané, J. Phys. Soc. Jpn. **72**, 1800 (2003).

[25] W. van Saarloos and P. C. Hohenberg, Phys. Rev. Lett. **64**, 749 (1990).

[26] K. Otsuka, *Nonlinear Dynamics in Optical Complex Systems* (KTK Scientific Publisher, Tokyo, 1999).

[27] N. K. Efremidis and D. N. Christodoulides, Phys. Rev. E **67**, 026606 (2003).

[28] B. P. Anderson and M. A. Kasevich, Science **282**, 1686 (1998).

[29] B. Kneer, T. Wong, K. Vogel, W. P. Schleich, and D. F. Walls, Phys. Rev. A **58**, 4841 (1998).

[30] F. T. Arecchi, J. Bragard, and L. M. Castellano, *in Bose-Einstein Condensates and Atom Lasers* (Kluwer, New York, 2002).

[31] J. D. Moores, Opt. Commun. **96**, 65 (1993).

[32] Y. Kodama, M. Romagnoli, and S. Wabnitz, Electron. Lett. **28**, 1981 (1992).

[33] H. A. Haus, J. G. Fujimoto, and E. P. Ippen, J. Opt. Soc. Am. B **8**, 2068 (1991).

[34] H. A. Haus, K. Tamura, L. E. Nelson, and E. P. Ippen, IEEE J. Quantum Electron. **31**, 591 (1995).

[35] C. G. Lange and A. C. Newell, SIAM J. Appl. Math. **27**, 441 (1974).

[36] A. Mohamadou, A. J. Kenfack, and T. C. Kofané, Chaos, Solitons Fractals **27**, 914 (2006).

[37] O. Descalzi, S. Martinez, and E. Tirapegui, Chaos, Solitons Fractals **12**, 2619 (2001).

[38] J. P. Nguenang, M. Peyrard, A. J. Kenfack, and T. C. Kofané, J. Phys.: Condens. Matter **17**, 3083 (2005); I. Daumont, T. Dauxois, and M. Peyrard, Nonlinearity **10**, 617 (1997).

[39] Yu. S. Kivshar and M. Peyrard, Phys. Rev. A **46**, 3198 (1992); A. Mohamadou, A. J. Kenfack, and T. C. Kofané, Phys. Rev. E **72**, 036220 (2005).

[40] J. S. Russell, in *Report on Waves, Proceedings of the 14th Meeting of the British Association for the Advancement of Science* (John Murray, London, 1844), pp. 311–390.

[41] N. R. Pereira and L. Stenflo, Phys. Fluids **20**, 1733 (1976); V. Filho, F. Kh. Abdullaev, A. Gammal, and L. Tomio, Phys. Rev. A **63**, 053603 (2001).

[42] V. M. Burlakov, Phys. Rev. Lett. **80**, 3988 (1998).